Preparation of a Pure Molecular Quantum Gas
Jens Herbig, *et al.*
Science **301**, 1510 (2003);
DOI: 10.1126/science.1088876

One additional correction that cannot be added as a σ in quadrature is the LMC rotation. Several young and intermediate-age kinematic tracers have been measured in the LMC, including HII regions, PN, CH stars, Miras, and carbon stars. In the inner regions of the LMC bar, these populations are rotating as a solid body, with 25 km/s per kpc. For a scale of 1 kpc = 1.2°, our fields should not show a rotation component larger than 10 km/s.

In addition, a correction for rotation may not be necessary for the RR Lyrae population, because there is no evidence that this old population follows the LMC rotation. On the basis of the Milky Way RR Lyrae, one might suspect that the LMC RR Lyrae do not rotate like the rest of the stars. However, a composite RR Lyrae population may be present. For example, earlier interpretation of the RR Lyrae number counts indicated an exponential disk distribution (*31*). Multiple components (halo plus thick disk) cannot be ruled out without rotation measurements. Our fields are not spread out enough to measure the rotation. In order to measure the systemic rotation of the RR Lyrae population, one would need to observe $N \cong 50$ stars per field in fields located >3° away on opposite sides of the bar. We estimate the correction in two ways: with the use of the velocities from HI maps (*32*) and with the use of the mean rotation fits of the disk (*22*, *24*). This correction does not change at all the LMC RR Lyrae velocity dispersion.

The large RR Lyrae velocity dispersion $\sigma_{true} = 53$ km/s implies that metal-poor old stars are distributed in a halo population. The velocity dispersion for the old RR Lyrae stars is higher than that for the old LMC clusters, although there are too few old clusters to measure the kinematics in the LMC. The presence of a kinematically hot, old, and metal-poor halo in the LMC suggests that galaxies like the Milky Way and small galaxies like the LMC have similar early formation histories (*33*).

The stellar halo traced by the RR Lyrae amounts only to 2% of the mass of the LMC, which is akin to the Milky Way halo (*1*, *22*). Consequently, its contribution to the microlensing optical depth should not be important (*26*, *34*). The ongoing Supermacho experiment will discover an order of magnitude more microlensing events toward the LMC (*35*), allowing us to test this prediction.

References and Notes

1. T. D. Kinman *et al.*, *Publ. Astron. Soc. Pac.* **103**, 1279 (1991).
2. M. Feast, in *Variable Stars and Galaxies*, Brian Warner, Ed. [Astronomical Society of the Pacific (ASP) Conference Series 30, San Francisco, 1992], p. 143.
3. E. W. Olszewski, N. B. Suntzeff, M. Mateo, *Annual Rev. Astron. Astrophys.* **34**, 511 (1996).
4. D. Minniti, *Astrophys. J.* **459**, 175 (1996).
5. A. Layden, in *Galactic Halos*, D. Zaritsky, Ed. (ASP Conference Series 136, San Francisco, 1998), p.14.
6. L. Searle, R. Zinn, *Astrophys. J.* **225**, 358 (1978).
7. O. Eggen, D. Lynden-Bell, A. Sandage, *Astrophys. J.* **136**, 748 (1962).
8. D. Minniti, A. A. Zijlstra, *Astrophys. J.* **467**, L13 (1996).
9. D. R. Alves, M. Rejkuba, D. Minniti, K. H. Cook, *Astrophys. J.* **573**, L51 (2002).
10. K. C. Freeman, G. Illingworth, A. Oemler, *Astrophys. J.* **272**, 488 (1983).
11. R. A. Schommer, E. W. Olszewski, N. B. Suntzeff, H. C. Harris, *Astron. J.* **103**, 447 (1992).
12. C. Alcock *et al.*, *Astrophys. J.* **490**, L59 (1997).
13. C. Alcock *et al.*, *Astrophys. J.* **482**, 89 (1997).
14. C. Alcock *et al.*, *Astrophys. J.* **542**, 257 (2000).
15. The MACHO RR Lyrae data are available online at the MACHO Project home page (www.macho.mcmaster.ca/). These RR Lyrae are classified on the basis of the MACHO light curves, with RRab being fundamental pulsators; RRc, first overtones; and RRe, double mode pulsators.
16. H. A. Smith, *The RR Lyrae Stars* (Cambridge Univ. Press, Cambridge, 1995).
17. C. M. Clement *et al.*, *Astron. J.* **122**, 2587 (2001).
18. M. Mayor *et al.*, *Astron. Astrophys.* **114**, 1087 (1997).
19. J. Kaluzny *et al.*, *Astron. Astrophys. Suppl. Ser.* **122**, 471 (1997).
20. J. E. Norris, K. C. Freeman, M. Mayor, P. Seitzer, *Astrophys. J.* **487**, 187 (1997).
21. D. S. Graff, A. Gould, N. B. Suntzeff, R. Schommer, E. Hardy, *Astrophys. J.* **540**, 211 (2000).
22. D. R. Alves, C. A. Nelson, *Astrophys. J.* **542**, 789 (2001).
23. E. Hardy, D. R. Alves, D. S. Graff, N. B. Suntzeff, R. A. Schommer, *Astrophys. J. Suppl. Ser.* **277**, 471 (2001).
24. R. P. van der Marel, D. R. Alves, E. Hardy, N. B. Suntzeff, *Astron. J.* **124**, 2639 (2002).
25. S. M. G. Hughes, P. R. Wood, I. N. Reid, *Astron. J.* **101**, 1304 (1991).
26. G. Gyuk, N. Dalal, K. Griest, *Astrophys. J.* **535**, 90 (2000).
27. We eliminated a low-velocity star, discrepant by more than 4σ from the mean, which could be a misidentified foreground star.
28. G. Clementini, R. Megighi, C. Cacciari, C. Gouiffes, *Mon. Not. R. Astron. Soc.* **267**, 83 (1994).
29. I. Skillen, J. A. Fernley, R. S. Stobie, R. F. Jameson, *Mon. Not. R. Astron. Soc.* **265**, 301 (1993).
30. We adopt a conservative error of 10 km/s for this quantity on the basis of uncertainties in the control samples.
31. C. Alcock *et al.*, *Astron. J.* **119**, 2194 (2000).
32. K. Rohlfs, J. Kreitschmann, B. C. Siegman, J. V. Feitzinger, *Astron. Astrophys.* **137**, 343 (1984).
33. The sample is not large enough and the velocities are not accurate enough to (i) detect tidal streams in front or behind the LMC and (ii) measure the systemic rotation of the halo RR Lyrae population. However, from a sample of this size, and with velocities measured to this accuracy, there is no difficulty in measuring the velocity dispersion and thus distinguishing a disk population from a halo population in the LMC.
34. C. Alcock *et al.*, *Astrophys. J.* **542**, 281 (2000).
35. C. Stubbs, in *The Galactic Halo*, B. K. Gibson, T. S. Axelrod, M. E. Putman, Eds. (ASP Conference Series 165, San Francisco, 2000), p. 503.

36. We gratefully acknowledge suggestions from E. Olszewski, A. Drake, M. Catelan, and C. Alcock and support by the Fondap Center for Astrophysics 15010003; by the U.S. Department of Energy National Nuclear Security Administration to University of California's Lawrence Livermore National Laboratory under contract W-7405-Eng-48; and by the Bilateral Science and Technology Program of the Australian Department of Industry, Technology, and Regional Development; and by ESO Program 70.B-0547.

27 June 2003; accepted 11 August 2003

Preparation of a Pure Molecular Quantum Gas

Jens Herbig, Tobias Kraemer, Michael Mark, Tino Weber, Cheng Chin, Hanns-Christoph Nägerl, Rudolf Grimm*

An ultracold molecular quantum gas is created by application of a magnetic field sweep across a Feshbach resonance to a Bose-Einstein condensate of cesium atoms. The ability to separate the molecules from the atoms permits direct imaging of the pure molecular sample. Magnetic levitation enables study of the dynamics of the ensemble on extended time scales. We measured ultralow expansion energies in the range of a few nanokelvin for a sample of 3000 molecules. Our observations are consistent with the presence of a macroscopic molecular matter wave.

Rapid progress in controlling ultracold atomic gases, culminating in the creation of atomic Bose-Einstein condensates (BECs) and opening the door to the realm of coherent matter-wave physics (*1*–*3*), has raised the question of whether a similar level of control is possible with molecular samples. Molecules, in contrast to atoms, have a much richer internal structure and can possess permanent vector or tensor properties, such as electric dipole moments, rotational angular momentum, and even chirality. Molecule-atom and molecule-molecule interactions are at least three- and four-body processes in nature, posing new challenges to our theoretical understanding. Exquisite control over the internal and external degrees of freedom of molecules could allow the experimental study of a new coherent chemistry (*4*), where matter-wave interference, quantum tunneling, and bosonic stimulation dominate the dynamics and where the interaction properties can be externally controlled and engineered with electromagnetic fields. Quantum degenerate molecular gases with permanent dipole moments are also prime candidates for the precise investigation of strongly correlated quantum

Institut für Experimentalphysik, Universität Innsbruck, Technikerstraβe 25, 6020 Innsbruck, Austria.

*To whom correspondence should be addressed. E-mail: rudolf.grimm@uibk.ac.at

systems and for the study of novel quantum phase transitions (*5*).

Several avenues have been investigated to cool and trap molecules. Slowing of a supersonic jet of polar molecules in time-varying electric fields (*6*) and buffer gas loading and trapping (*7*) in either electrostatic or magnetic traps both permit large molecular populations with temperatures in the mK range. Alternatively, creation of molecules by photoassociation of precooled atoms has led to molecular samples with temperatures in the μK range (*8*). For all these techniques, however, the resulting molecular phase-space density is still many orders of magnitude away from quantum degeneracy.

Starting with a sample of ultracold atoms, controlled production of molecules can be realized by the coherent coupling of an atom pair state to a molecular state. For example, a two-photon Raman transition has successfully been applied to produce molecules within an atomic BEC (*9*). Similarly, the coherent nature of atomic scattering can be exploited on a Feshbach resonance to transfer colliding atoms into molecules, which has been predicted to convert an atomic BEC into a molecular BEC (*10*–*12*). A Feshbach resonance occurs when the energy of the atomic scattering state is tuned into degeneracy with that of a bound molecular state (*13*). Experimentally, Feshbach resonances can be induced by an external magnetic field when both states feature different Zeeman shifts. Consequently, the atom-molecule coupling can be resonantly enhanced at a particular magnetic field value, and a sweep of the field near or across the resonance can convert the atoms into molecules in a single molecular quantum state. Existence of molecules created through atomic Feshbach resonances has been reported previously in a BEC of ^{85}Rb atoms (*14*), in thermal samples of ^{133}Cs (*15*), and in degenerate Fermi gases of ^{40}K (*16*) and ^{6}Li (*17*). These studies demonstrate the quantum coherence of the Feshbach coupling (*14*) and the ability to detect molecules within the atomic sample by means of laser-induced (*15*) or radiofrequency-induced (*16*) dissociation. However, the resulting molecular samples could not be spatially distinguished from the atoms, nor could the molecular clouds be directly imaged and analyzed. Here, we report the observation of pure molecular quantum matter, achieved by applying a Feshbach sweep to an atomic Cs BEC (*18*) with immediate spatial Stern-Gerlach separation of the two species. By monitoring the evolution of the coupled-out molecular cloud, we measure ultralow kinetic expansion energies that are consistent with the presence of a coherent molecular matter wave.

The starting point of our experiment was a pure BEC of up to 6×10^4 Cs atoms in an optical trap (*19*) with a radial Thomas-Fermi radius of 8.6 μm and an axial Thomas-Fermi radius of 26.5 μm. The atoms were in the hyperfine ground state with total angular momentum $F = 3$ and magnetic quantum number $m_F = 3$. As the optical trap was by far too weak to support the atoms against gravity during the evaporative cooling process, a magnetic field gradient of 30.9 G/cm was applied to levitate the atoms (*20*). This levitation is very sensitive to the magnetic moment of the trapped particles, and a small change of 1% in either the gradient or in the magnetic moment of the trapped particles is sufficient to render the trap unstable. The state $F = 3$, $m_F = 3$ features a narrow Feshbach resonance near 20 G (*21*) with an estimated resonance width of 5 mG (*22*). According to an analysis of the Cs scattering properties (*23*, *24*), the corresponding molecular state (*25*) has a predicted magnetic moment of $\mu = 0.93\ \mu_B$, where μ_B is Bohr's magneton, with a small magnetic field dependence (*22*). We produced molecules from the atomic BEC by sweeping the magnetic field across the resonance from a higher field value with a constant rate of typically 50 G/s (Fig. 1). The duration of the sweep was 3 ms. To turn off the Feshbach coupling, the field was then quickly lowered to a hold field at 17 G for a variable hold time while the optical trap was shut off (*20*). Because of the large magnetic field gradient along the vertical direction and the narrow resonance width of 5 mG, the Feshbach resonance occurred only within a 2-μm-thin horizontal layer. The conversion zone swept through the condensate from below at a speed of 15 μm/ms, or equivalently, in 1.3 ms. The newly created molecules immediately started falling with an acceleration of 0.38*g* due to their reduced magnetic moment. The molecular cloud was then completely separated from the atoms within 3 ms. By raising the magnetic field gradient quickly at the end of the sweep to about 50 G/cm, we levitated the molecules. In this case, the atoms accelerated upward at 0.61*g*. Rapid molecule-atom separation and subsequent levitation permit long observation times for studying the dynamics of the molecular sample.

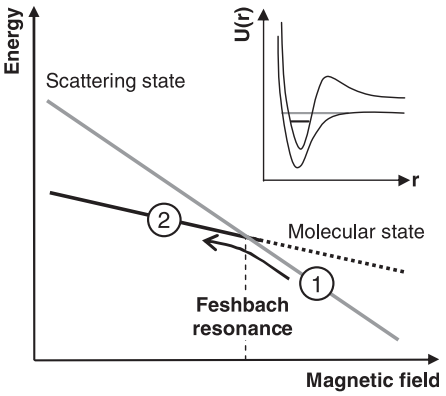

Fig. 1. Energy diagram for the atomic scattering state and the molecular bound state. The Feshbach resonance condition occurs near 20 G, where the Zeeman energy of the atomic scattering state becomes equal to that of a molecular bound state because of the difference in magnetic moments. Molecules at (2) are created from the BEC at (1) by a downward sweep of the magnetic field across the resonance. For detection, a reversed sweep brings the molecules above the dissociation limit. The inset schematically shows the molecular potential that corresponds to the open channel (lower curve) and the molecular potential that supports the bound state (upper curve). U, potential energy; r, interatomic distance.

To image the molecular cloud, we applied a reversed field sweep across the Feshbach resonance. The reversed sweep brought the molecules above the scattering continuum, and they quickly dissociated into free atoms. An immediate absorption image of the reconverted atoms thus reveals the spatial distribution of the molecules. A resolution limit of about 10 μm was caused by an energy on the order of $k_B \times 1$ μK released in the dissociation process (*20*), where k_B is the Boltzmann constant. We applied a fit to the image to determine the center position, the size of the spatial distribution, and the number of molecules. The evolution of the molecular cloud was recorded by variation of the hold time.

The complete atom-molecule separation is clearly visible in absorption images (Fig. 2). For reference, the image of a levitated BEC after 12 ms of expansion time is given in Fig. 2A. In Fig. 2, B and C, a Feshbach sweep has been applied to the BEC. In Fig. 2B, a coupled-out molecular cloud with ~3000 molecules can be seen below the atomic BEC. The number of atoms in the remaining BEC is reduced by 50% from those shown in Fig. 2A, to ~25,000. The molecular cloud is falling, because the magnetic field gradient needed to levitate the atoms was maintained. For Fig. 2C, the magnetic field gradient was

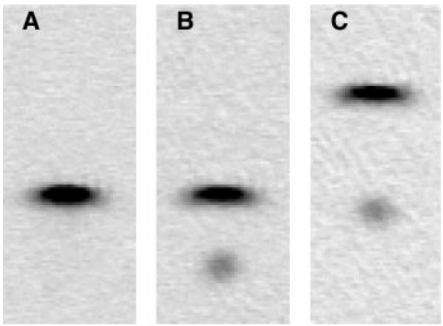

Fig. 2. Absorption images of (**A**) the levitated BEC without the Feshbach sweep, (**B**) the levitated BEC after the Feshbach sweep with a falling molecular cloud below, and (**C**) the levitated molecular cloud with an upward-rising BEC above. In (B) and (C), 3000 molecules are produced at a sweep rate of 50 G/s. The separation between the atoms and the molecules is 150 μm in (B) and 240 μm in (C).

raised after the Feshbach sweep in order to levitate the molecules. Hence, the atomic BEC accelerates upward and can be seen at the top of the image above the molecules. Careful adjustment of the magnetic field gradient to null the molecular acceleration allowed a precise determination of the molecular magnetic moment. We find that $\mu = 0.930(5)\ \mu_B$ (*20*), which is in good agreement with the theoretical calculation (*22*).

We investigated the atom-molecule conversion as a function of the end value B_f of the creation ramp. The ramp speed was kept constant at 50 G/s by variation of B_f together with the duration of the ramp. We have checked that for final values of B_f well above the resonance, the rapid jump over the resonance to the hold field after the end of the creation ramp did not produce any molecules. As Fig. 3 shows, molecules were created in a steplike manner. Simultaneously, the atomic population in the BEC is reduced. The transition value agrees well with the resonance position of 19.83(2) G as determined from three-body recombination loss measurements (*26*). From the plot of the atom number, it can be seen that up to 50% of the atoms were lost from the condensate, corresponding to ~25,000 atoms for this experiment. Hence, for a detected number of 3000 molecules, only about 24% of the lost atoms reappeared as partners in molecule formation. Also, we varied the speed of the downward magnetic field ramp across the Feshbach resonance and found that for decreasing ramp speed, the number of detected molecules saturated at a value of ~3000 molecules for speeds less than 50 G/s. The missing atoms and the saturation suggest that collisional relaxation into other molecular states occurs during the creation phase (*27*). After separation from the atoms, however, we did not detect any substantial loss.

We observed ultralow expansion energies for the molecular cloud in both the vertical and the horizontal directions. This was done in time-of-flight expansion measurements by variation of the hold time and hence the total expansion time. We plotted the vertical and horizontal root-mean-square (rms) widths of the reconverted atomic cloud as a function of total expansion time (Fig. 4, A and B). An apparent anisotropy of the expansion can be seen. The faster vertical expansion corresponds to a mean kinetic energy of $E_z = \frac{1}{2}\ k_B \times (40 \pm 3 \pm 2)$ nK (*20*), where the first one-standard-deviation error is statistical and the second one is systematic. The origin of this vertical energy was identified as the velocity dispersion of the molecules during the creation phase. The dispersion was caused by the fact that the conversion zone passes through the condensate at a finite speed from below. Hence, molecules created earlier acquire a larger velocity, and those created later acquire a smaller velocity, as a result of the gravity pulling. When the size of the BEC was taken into account, the vertical expansion energy as a result of the velocity dispersion was calculated to be about $\frac{1}{2}\ k_B \times 30$ nK for the molecular cloud, largely explaining the observed energy. In fact, vertical compression of the BEC did lead to a smaller vertical energy spread. By increasing the dipole trap depth to decrease the vertical extent of the BEC by a factor of 1.3, we found that the measured molecular kinetic energy was reduced in the expected way to a value of $E_z = \frac{1}{2}\ k_B \times (19 \pm 2 \pm 1)$ nK.

The horizontal expansion shown in Fig. 4B was unaffected by the velocity dispersion effect. However, a repulsive force due to the curvature of the levitation field acted on the molecules. This force resulted in an expansion of the cloud that follows a cosine hyperbolicus function and has been characterized previously (*18*). When the resolution limit due to the dissociation and the cosine hyperbolicus expansion dynamics (*20*) is incorporated, the fit in Fig. 4B yields an extremely low kinetic energy of $E_x = \frac{1}{2}\ k_B \times (2 \pm 2 \pm 3)$ nK in the horizontal direction.

The slow expansion of the molecules is consistent with the behavior of a macroscopic matter wave, as the horizontal expansion showed vanishing release energy and the vertical expansion was dominated by the dispersive gravity pulling effect, which is coherent in its nature. In view of a possible quantum degeneracy of the molecular ensemble, we first estimated the peak molecular density right after creation to $1 \times 10^{12}\ \mathrm{cm}^{-3}$, assuming 3000 molecules with a spatial density profile that reflects that of the atomic BEC (*28*). Given the free-space degeneracy condition, the critical temperature is 6 nK. Comparing this value to the observed horizontal energy spread that corresponds to $(2 \pm 2 \pm 3)$ nK, we raise the question whether a molecular cloud with macroscopic coherence has been created. Our capability to monitor the spatial distribution of the molecules should allow us to detect interference patterns (*29*) and thus to investigate the macroscopic coherence of the molecular matter wave.

To create molecules coherently with high efficiency, it will be advantageous to load the atomic BEC into an optical lattice (*30*), which allows the preparation of a Mott insulator phase (*31*) with exactly two atoms per lattice site. Molecules created by a subsequent Feshbach sweep will therefore be individually isolated and immune to collisional losses. After the creation of a pure molecular matter wave, one might be able to coherently transfer the molecules to low-lying molecular states by two-photon Raman transitions. Hence, a complete and coherent control over the dynamics of molecular quantum matter can be envisaged.

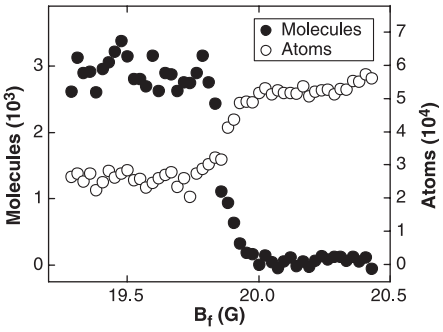

Fig. 3. Creation of molecules (solid circles) and simultaneous loss of atoms (open circles) as a function of the final value of the magnetic field ramp B_f for a fixed ramp speed of 50 G/s.

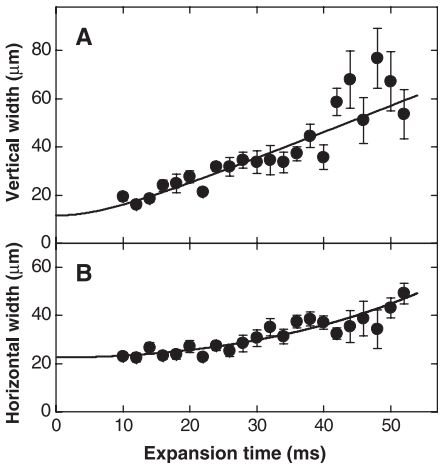

Fig. 4. (**A**) Vertical rms width and (**B**) horizontal rms width of the molecular cloud as a function of expansion time. From (A), a vertical expansion energy of $E_z = 1/2\ k_B \times (40 \pm 3 \pm 2)$ nK and an imaging resolution of 11(3) μm is obtained. The fit in (B) then yields an initial horizontal expansion energy of $E_x = 1/2\ k_B \times (2 \pm 2 \pm 3)$ nK.

References and Notes

1. E. A. Cornell, C. E. Wieman, *Rev. Mod. Phys.* **74**, 875 (2002).
2. W. Ketterle, *Rev. Mod. Phys.* **74**, 1131 (2002).
3. Nature Insight on Ultracold Matter, *Nature* **416**, 205 (2002).
4. D. J. Heinzen, R. Wynar, P. D. Drummond, K. V. Kheruntsyan, *Phys. Rev. Lett.* **84**, 5029 (2000).
5. K. Góral, L. Santos, M. Lewenstein, *Phys. Rev. Lett.* **88**, 170406 (2002).
6. H. L. Bethlem *et al.*, *Nature* **406**, 491 (2000).
7. J. D. Weinstein, R. deCarvalho, T. Guillet, B. Friedrich, J. M. Doyle, *Nature* **395**, 148 (1998).
8. N. Vanhaecke, W. de Souza Melo, B. L. Tolra, D. Comparat, P. Pillet, *Phys. Rev. Lett.* **89**, 063001 (2002).
9. R. Wynar, R. S. Freeland, D. J. Han, C. Ryu, D. J. Heinzen, *Science* **287**, 1016 (2000).
10. F. A. van Abeelen, B. J. Verhaar, *Phys. Rev. Lett.* **83**, 1550 (1999).
11. E. Timmermans, P. Tommasini, M. Hussein, A. Kerman, *Phys. Rep.* **315**, 199 (1999).
12. F. H. Mies, E. Tiesinga, P. S. Julienne, *Phys. Rev. A* **61**, 022721 (2000).
13. S. Inouye *et al.*, *Nature* **392**, 151 (1998).
14. E. A. Donley, N. R. Claussen, S. T. Thompson, C. E. Wieman, *Nature* **417**, 529 (2002).
15. C. Chin, A. J. Kerman, V. Vuletić, S. Chu, *Phys. Rev. Lett.* **90**, 033201 (2003).
16. C. A. Regal, C. Ticknor, J. L. Bohn, D. S. Jin, *Nature* **424**, 47 (2003).

17. C. Salomon, talk presented at the Quantum Electronics and Laser Science Conference, Baltimore, MD, 5 June 2003.
18. T. Weber, J. Herbig, M. Mark, H.-C. Nägerl, R. Grimm, *Science* **299**, 232 (2003); published online 5 Dec 2002 (10.1126/science.1079699).
19. The optical trap has a depth of $k_B \times 45$ nK with a radial trap frequency of 18 Hz and an axial trap frequency of 6 Hz. The axial direction of the BEC is oriented in the horizontal plane. At 20 G, the Cs scattering length is $a = 163\ a_0$, with a_0 denoting Bohr's radius. The resulting chemical potential for the BEC is $k_B \times 7$ nK.
20. Materials and methods are available as supporting material on *Science* Online.
21. V. Vuletić, C. Chin, A. J. Kerman, S. Chu, *Phys. Rev. Lett.* **83**, 943 (1999).
22. P. S. Julienne, E. Tiesinga, private communication (2003).
23. C. Chin, V. Vuletić, A. J. Kerman, S. Chu, *Phys. Rev. Lett.* **85**, 2717 (2000).
24. P. J. Leo, C. J. Williams, P. S. Julienne, *Phys. Rev. Lett.* **85**, 2721 (2000).
25. The molecular state was identified as a high-lying rovibrational state with internal angular momentum $f = 4$, magnetic quantum number $m_f = 4$, molecular orbital angular momentum $L = 4$, and angular momentum projection $m_L = 2$.
26. T. Weber, J. Herbig, M. Mark, H.-C. Nägerl, R. Grimm, *Phys. Rev. Lett.*, in press (available at http://arXiv.org/abs/physics/0304052).
27. V. A. Yurovsky, A. Ben-Reuven, P. S. Julienne, C. J. Williams, *Phys. Rev. A* **62**, 043605 (2000).
28. This is a reasonable assumption, because no molecules can be created in the absence of atoms.
29. M. R. Andrews *et al.*, *Science* **275**, 637 (1997).
30. D. Jaksch, V. Venturi, J. I. Cirac, C. J. Williams, P. Zoller, *Phys. Rev. Lett.* **89**, 040402 (2002).
31. M. Greiner, O. Mandel, T. Esslinger, T. W. Hänsch, I. Bloch, *Nature* **415**, 39 (2002).
32. We thank P. S. Julienne for very helpful discussions. Supported by the Austrian Science Fund (FWF) within Spezialforschungsbereich 15 (project part 16) and by the European Union through the Cold Molecules Training and Mobility of Researchers Network under contract no. HPRN-CT-2002-00290.

Supporting Online Material
www.sciencemag.org/cgi/content/full/1088876/DC1
Materials and Methods
Figs. S1 to S3

7 July 2003; accepted 11 August 2003
Published online 21 August 2003;
10.1126/science.1088876
Include this information when citing this paper.

Cooling Bose-Einstein Condensates Below 500 Picokelvin

A. E. Leanhardt,* T. A. Pasquini, M. Saba, A. Schirotzek, Y. Shin, D. Kielpinski, D. E. Pritchard, W. Ketterle

Spin-polarized gaseous Bose-Einstein condensates were confined by a combination of gravitational and magnetic forces. The partially condensed atomic vapors were adiabatically decompressed by weakening the gravito-magnetic trap to a mean frequency of 1 hertz, then evaporatively reduced in size to 2500 atoms. This lowered the peak condensate density to 5×10^{10} atoms per cubic centimeter and cooled the entire cloud in all three dimensions to a kinetic temperature of 450 ± 80 picokelvin. Such spin-polarized, dilute, and ultracold gases are important for spectroscopy, metrology, and atom optics.

The pursuit of lower temperatures is motivated by the quest to observe phenomena that occur on very low energy scales, in particular, phase transitions to new forms of matter. The achievement of temperatures near 1 K in solids and in liquids led to the discoveries of superconductivity (*1*) and superfluidity (*2*), respectively. The advent of laser cooling resulted in microkelvin temperature atomic vapors (*3*–*5*), subsequently cooled to nanokelvin temperatures by evaporative cooling to form dilute Bose-Einstein condensates (*6*, *7*) and quantum degenerate Fermi gases (*8*). Collectively, these low-temperature systems have a host of applications, including superconducting quantum interference devices (SQUIDs) (*9*), superfluid gyroscopes (*10*, *11*), and atomic clocks (*12*).

Temperature is a quantity that parameterizes how energy is distributed across the available states of a system, and effective temperatures can be defined for decoupled degrees of freedom or subsets of particles. For example, nuclear spins isolated from the kinetic motion of their respective atoms have been cooled by adiabatic demagnetization to an effective temperature of 280 pK (*13*). Spin ensembles have a finite number of available states, such that a spin-polarized sample, as in our work, would be characterized by zero effective temperature. In contrast, the motion of free particles is subject to a continuum of states, and the kinetic temperature of an ensemble can only asymptotically approach absolute zero.

Effective temperatures in atomic vapors are defined by the widths of velocity distributions, which can be much smaller than the mean velocity of the sample. Raman cooling (*14*, *15*) and velocity-selective coherent population trapping (VSCPT) (*16*) have generated velocity distributions with very narrow peaks, corresponding to nanokelvin and picokelvin effective temperatures. However, these temperatures were associated with the motion of only a subset of the atoms in the cloud and/or with atomic motion in only one dimension.

For trapped, partially condensed atomic vapors, the condensate fraction has zero entropy and the kinetic temperature of the sample is determined by the velocity distribution of the thermal (noncondensed) component. When released, the condensate fraction expands more slowly than the thermal component and has been characterized by picokelvin effective temperatures for anisotropic (*17*) and noninteracting (*18*) gases.

Cooling the atomic motion of entire ensembles in all three dimensions has proven difficult. To date, kinetic temperatures of a few hundred nanokelvin have been achieved with adiabatic and optical cooling (*19*, *20*), and evaporative cooling techniques have produced condensates with temperatures of 3 nK (*21*). By adiabatic expansion and subsequent evaporation, we have cooled partially condensed atomic vapors to picokelvin kinetic temperatures.

Our thermometry is calibrated by the Bose-Einstein condensation (BEC) phase transition temperature, T_c, which in the thermodynamic limit for a harmonically trapped ideal Bose gas is (*22*)

$$k_B T_c = \hbar\bar{\omega}\left(\frac{N}{\zeta(3)}\right)^{1/3} \approx 0.94\hbar\bar{\omega}N^{1/3} \qquad (1)$$

where k_B is Boltzmann's constant, $\hbar$ is Planck's constant h divided by 2π, $\zeta(n)$ is the Riemann Zeta function, $\bar{\omega} = (\omega_x\omega_y\omega_z)^{1/3}$ is the geometric mean of the harmonic trap frequencies, and N is the total number of atoms, both condensed and noncondensed. Thus, the atom number and the trap frequencies set an upper limit for the temperature of a confined Bose-Einstein condensate. In our work, adiabatically weakening the trapping potential to a mean frequency of $\bar{\omega} = 2\pi \times (1.12 \pm 0.08)$ Hz guaranteed that partially condensed atomic vapors with $N \leq 8000$ atoms had picokelvin temperatures ($T_c \leq 1$ nK).

Bose-Einstein condensates containing more than 10^7 ^{23}Na atoms were created in the weak field seeking $|F = 1, m_F = -1\rangle$ state in a magnetic trap, captured in the focus of an optical tweezers laser beam, and transferred into an auxiliary "science" chamber as described in (*23*). In the science chamber, condensates containing 2×10^6 to 3×10^6 atoms were transferred from the optical tweezers into a gravito-magnetic trap (Fig. 1A). A small coil carrying current I_S generated a vertical bias field B_z and supported the condensates against gravity with a vertical magnetic field gradient, $B'_z = 2\ mg/$

Department of Physics, MIT-Harvard Center for Ultracold Atoms, and Research Laboratory of Electronics, Massachusetts Institute of Technology, Cambridge, MA 02139, USA.

*To whom correspondence should be addressed. E-mail: ael@mit.edu